Supplementary Information

Ion-induced diversity in structure and magnetic properties of hexacyanometalate-lanthanide bimetallic assemblies

Mohd. Muddassir, Xiao-Jiao Song, Ying Chen, Fan Cao, Rong-Min Wei, You Song*

Table S1. Selected bond lengths (Å) and angles (°) for **2** and **4**.

2		**4**	
Dy1—O1	2.294 (5)	Ho1—O1	2.358 (3)
Dy1—O2	2.279 (4)	Ho1—O2	2.325 (3)
Dy1—O3	2.323 (4)	Ho1—O3	2.322 (3)
Dy1—N1	2.448 (5)	Ho1—N4	2.394 (4)
Dy1—N2	2.497 (5)	Ho1—N9i	2.438 (4)
Dy1—N3	2.524 (6)	Ho1—N1	2.464 (4)
Dy1—N4	2.445 (5)	Ho1—N3	2.466 (4)
Dy1—N5^{i}	2.400 (5)	Ho1—N2	2.476 (4)
N5—Dy1^{ii}	2.400 (5)	N9—Ho1i	2.438 (4)
C16—Co1	1.868 (6)	C16—Co1	1.879 (5)
C17—Co1	1.892 (7)	C17—Co1	1.910 (5)
C18—Co1	1.903 (6)	C18—Co1	1.896 (5)
C19—Co1	1.863 (7)	C19—Co1	1.889 (5)
C20—Co1	1.893 (7)	C20—Co1	1.877 (5)
C21—Co1	1.886 (7)	C21—Co1	1.917 (5)
O2—Dy1—O1	82.38 (19)	O3—Ho1—O2	70.87 (12)
O2—Dy1—O3	91.52 (17)	O3—Ho1—O1	144.49 (12)
O1—Dy1—O3	143.42 (18)	O2—Ho1—O1	144.18 (11)
O2—Dy1—N5i	90.92 (17)	O3—Ho1—N4	77.80 (13)
O1—Dy1—N5i	71.79 (18)	O2—Ho1—N4	103.89 (13)
O3—Dy1—N5i	144.63 (17)	O1—Ho1—N4	85.06 (14)
O2—Dy1—N4	78.65 (16)	O3—Ho1—N9i	74.57 (12)
O1—Dy1—N4	73.96 (18)	O2—Ho1—N9i	143.36 (12)
O3—Dy1—N4	69.48 (15)	O1—Ho1—N9i	71.94 (12)
N5i—Dy1—N4	145.22 (17)	N4—Ho1—N9i	79.94 (13)
O2—Dy1—N1	151.66 (18)	O3—Ho1—N1	128.32 (12)
O1—Dy1—N1	77.29 (19)	O2—Ho1—N1	70.06 (12)
O3—Dy1—N1	93.15 (17)	O1—Ho1—N1	77.68 (12)
N5i—Dy1—N1	101.10 (17)	N4—Ho1—N1	80.16 (14)
N4—Dy1—N1	76.90 (17)	N9i—Ho1—N1	144.81 (14)
O2—Dy1—N2	140.78 (18)	O3—Ho1—N3	81.97 (13)
O1—Dy1—N2	129.04 (18)	O2—Ho1—N3	89.65 (13)
O3—Dy1—N2	75.66 (16)	O1—Ho1—N3	99.47 (13)
N5i—Dy1—N2	80.34 (17)	N4—Ho1—N3	150.21 (13)
N4—Dy1—N2	127.64 (16)	N9i—Ho1—N3	73.70 (13)

N1—Dy1—N2	67.18 (19)	N1—Ho1—N3	129.62 (14)
O2—Dy1—N3	76.45 (19)	O3—Ho1—N2	135.84 (13)
O1—Dy1—N3	136.65 (19)	O2—Ho1—N2	79.99 (12)
O3—Dy1—N3	75.13 (17)	O1—Ho1—N2	72.94 (12)
N5i—Dy1—N3	71.20 (17)	N4—Ho1—N2	142.75 (13)
N4—Dy1—N3	135.67 (18)	N9i—Ho1—N2	119.08 (13)
N1—Dy1—N3	131.7 (2)	N1—Ho1—N2	66.20 (13)
N2—Dy1—N3	64.5 (2)	N3—Ho1—N2	65.07 (13)
C1—N1—Dy1	123.6 (5)	C1—N1—Ho1	122.2 (3)
C5—N1—Dy1	118.5 (5)	C5—N1—Ho1	119.4 (3)
C11—N3—Dy1	120.3 (5)	C6—N2—Ho1	120.1 (3)
C6—N2—Dy1	120.0 (5)	C10—N2—Ho1	118.7 (3)
C10—N2—Dy1	121.7 (5)	C15—N3—Ho1	122.2 (3)
C19—N4—Dy1	164.7 (5)	C11—N3—Ho1	120.3 (3)
C16—N5—Dy1^{ii}	158.6 (5)	C16—N4—Ho1	163.0 (4)
C25B—O1—Dy1	147.1 (12)	C20—N9—Ho1i	160.4 (4)
C22—O2—Dy1	138.4 (5)	C22—O3—Ho1	133.4 (3)
C19—Co1—C16	93.9 (2)	C19—Co1—C18	89.6 (2)
C19—Co1—C21	88.1 (3)	C20—Co1—C17	89.83 (19)
C16—Co1—C21	91.4 (3)	C16—Co1—C17	91.5 (2)
C19—Co1—C17	176.4 (3)	C19—Co1—C17	176.87 (19)
C16—Co1—C17	89.2 (2)	C18—Co1—C17	88.6 (2)
C21—Co1—C17	90.1 (3)	C20—Co1—C21	176.5 (2)
C19—Co1—C20	89.5 (3)	C16—Co1—C21	87.49 (19)
C16—Co1—C20	88.4 (2)	C19—Co1—C21	90.08 (19)
C21—Co1—C20	177.6 (3)	C18—Co1—C21	91.1 (2)
C17—Co1—C20	92.3 (3)	C17—Co1—C21	92.49 (19)
C19—Co1—C18	88.2 (2)	N4—C16—Co1	177.4 (4)
C16—Co1—C18	177.5 (3)	N5—C17—Co1	178.8 (4)
C21—Co1—C18	89.9 (3)	N6—C18—Co1	178.2 (4)
C17—Co1—C18	88.8 (3)	N7—C19—Co1	176.0 (4)
C20—Co1—C18	90.4 (3)	N9—C20—Co1	178.1 (4)
N5—C16—Co1	175.7 (6)	N8—C21—Co1	176.6 (5)
N6—C17—Co1	177.8 (6)	C20—Co1—C16	89.88 (19)
N7—C18—Co1	179.8 (7)	C20—Co1—C19	87.68 (19)
N4—C19—Co1	173.0 (5)	C16—Co1—C19	90.44 (19)
N9—C20—Co1	177.3 (6)	C20—Co1—C18	91.51 (19)
N8—C21—Co1	178.4 (6)	C16—Co1—C18	178.61 (19)

Symmetry codes: (i) x, −y+3/2, z−1/2; (ii) −x, −y+1, −z+2.

Table S2. Results of the SHAPE analysis for the Lanthenides in compounds **1-4.**

Structure [Ln]	(SAPR-8)[a]	(DD-8)[a]	(BTP-8)[a]
1	3.212788	1.369765	2.248511
2	3.171696	1.329167	2.238741
3	1.314185	1.701814	2.301209
4	1.316390	1.678959	2.401612

[a]SAPR-8: D_{4d}, Square antiprism; DD-8: D_{2d}, Triangular dodecahedron; BTP-8: D_{3d}, Bicapped trigonal prism.

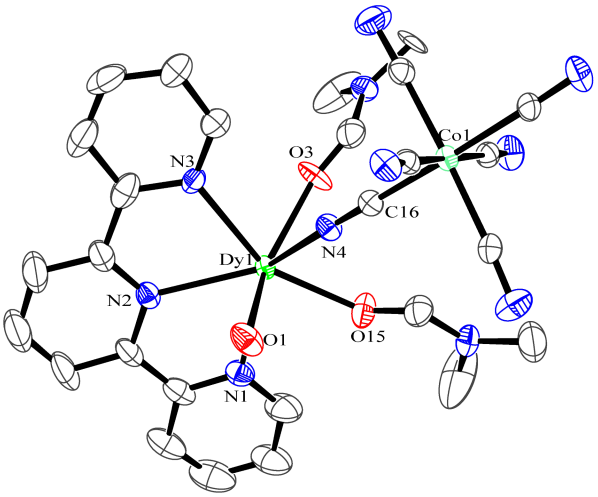

Fig. S1**.** ORTEP plot of **2** showing coordination environment of Dy^{III} and Co^{III} (thermal ellipsoids are drawn at the 30% probability level). H-atoms, disordered atoms, lattice water and methanol have been omitted for clarity.

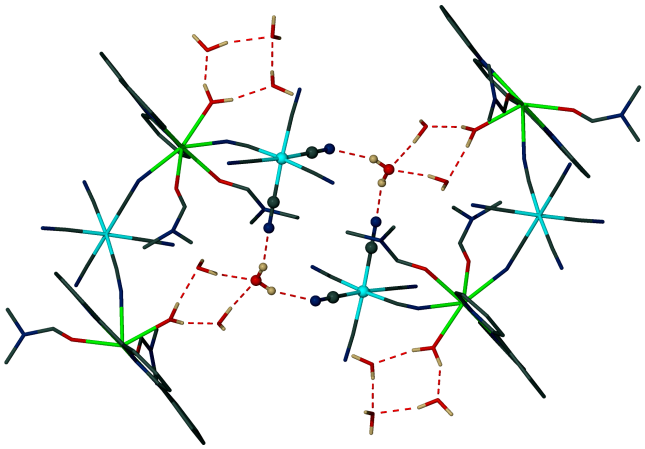

Fig. S2**.** Arrangement of 16-membered ring in **1** (projecting down *b*-axis) formed by O−H---N bonding between adjacent 1D chains generating a double buckled chain. Atoms involving in 16-membered ring are shown as spheres of arbitrary radii.

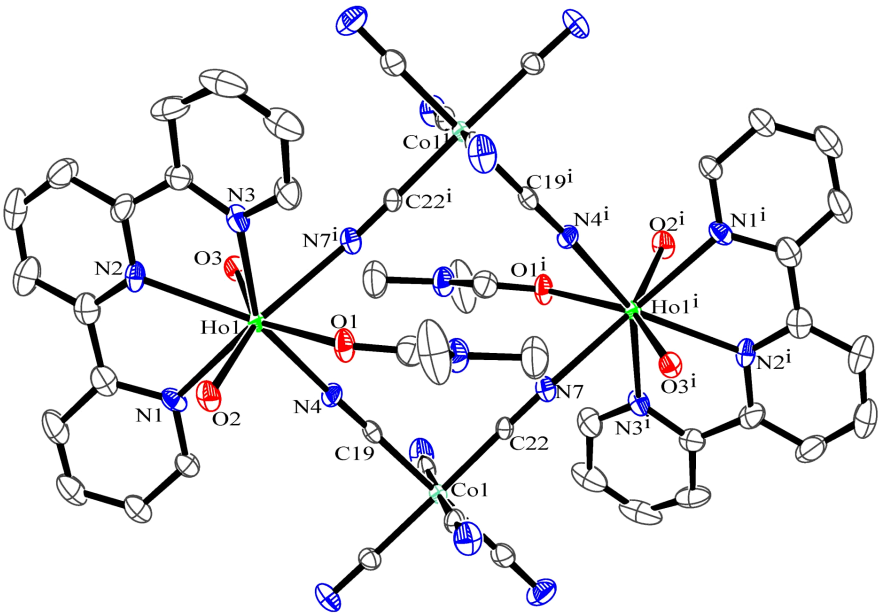

Fig. S3**.** The molecular structure of **4**, showing 30% probability ellipsoids displacement level H-atoms, disordered atoms and lattice water have been omitted for clarity.

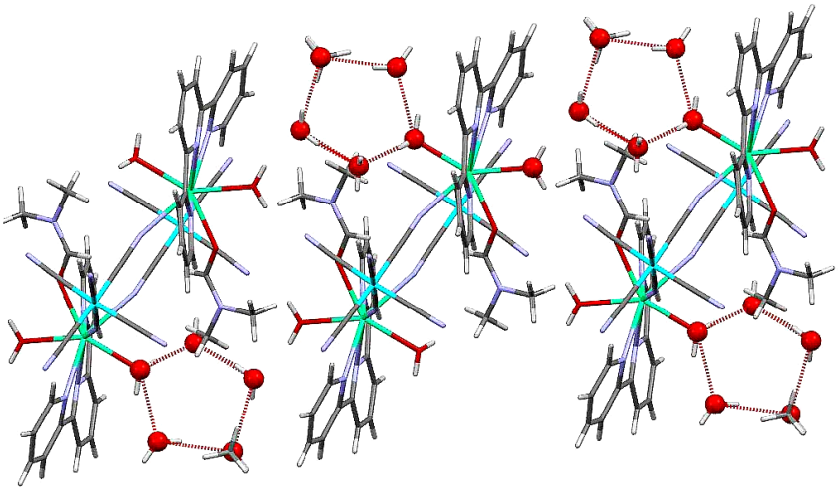

Fig. S4**.**1-D zigzag chain of **3** running parallel to *bc*-plane. O (red) of water and methanol atoms are shown as spheres of arbitrary radii.

Table S3. Hydrogen bonds for complex 1–4.

Complex 1

Donor	--- H....	Acceptor	D...A
O(4)	--H(4A)	..O(3)	2.710(4)
O(5)	--H(5B)	..O(3)	2.574(4)
O(6)	--H(6A)	..O(4)	2.811(4)
O(6)	--H(6B)	..O(5)	2.763(5)
O(5)	--H(5B)	..N(6)	2.756(4)
O(6)	--H(6A)	..N(9)	2.861(4)
O(6)	--H(6B)	..N(7)	2.792(4)

Complex 2

Donor	--- H....	Acceptor	D...A
O(4)	--H(4A)	..O(3)	2.688(4)
O(5)	--H(5B)	..O(3)	2.561(4)
O(6)	--H(6A)	..O(4)	2.829(4)
O(6)	--H(6B)	..O(5)	2.758(5)
O(5)	--H(5B)	..N(6)	2.761(4)
O(6)	--H(6A)	..N(9)	2.841(4)
O(6)	--H(6B)	..N(7)	2.802(4)

Complex 3

Donor	--- H....	Acceptor	D...A
O(2)	--H(2A)	..O(4)	2.732(8)
O(4)	--H(4B)	.. O(6)	2.867(8)
O(4)	--H(4B)	.. O(8)	2.979(8)
O(8)	--H(8A)	.. O(5)	2.869(7)
O(5)	--H(5A)	.. O(1)	2.735(8)
O(5)	--H(5B)	..N(8)	2.860(7)
O(2)	--H(2B)	..N(7)	2.728(7)

Complex 4

Donor	--- H....	Acceptor	D...A
O(2)	--H(2A)	..O(4)	2.768(8)
O(4)	--H(4B)	.. O(6)	2.812(8)
O(4)	--H(4B)	.. O(7)	2.739(8)
O(7)	--H(8A)	.. O(5)	2.849(7)
O(5)	--H(5A)	.. O(1)	2.746(8)
O(5)	--H(5B)	..N(8)	2.865(7)
O(2)	--H(2B)	..N(7)	2.723(7)

(a)

(b)

(c)

(d)

Fig. S5**.** FTIR spectra of complexes **1**-**4** (a-d).

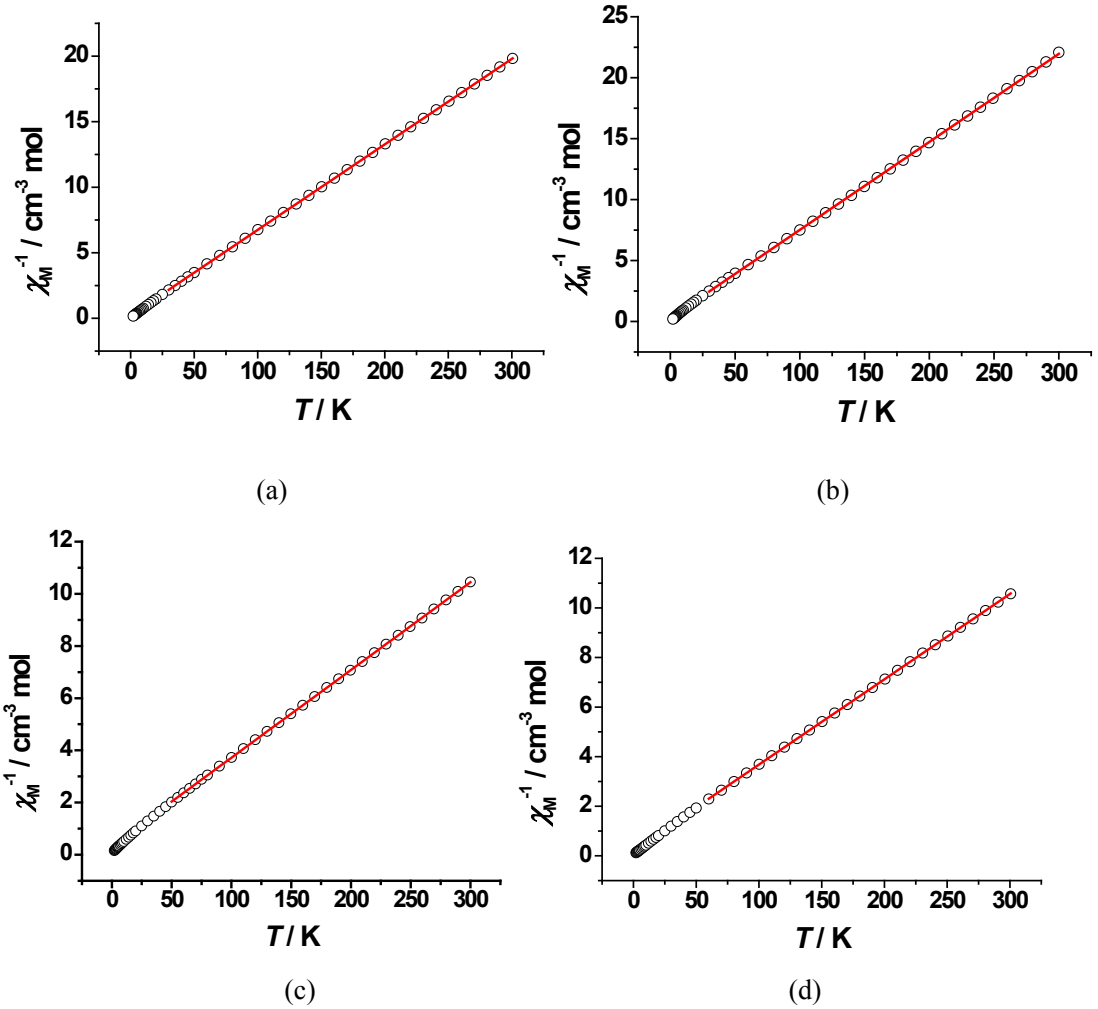

Fig. S6. Plot of χ_M^{-1} vs T for complex **1**-**4** (a-d) at 0.1 kOe applied field with the linear fit shown as a red line.

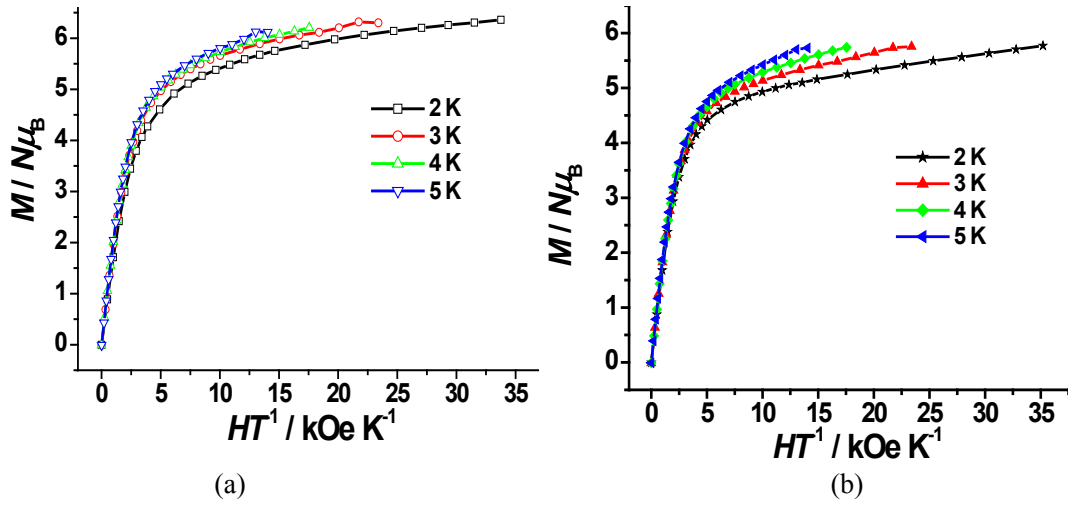

Fig. S7. M vs H/T plots at different temperatures **1**(a) and **2**(b).

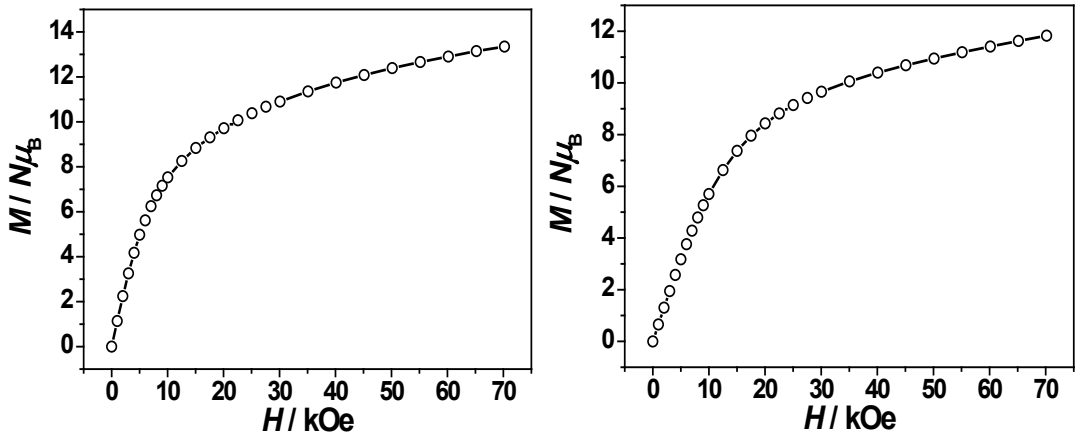

Fig. S8**.** The curve of field-dependent magnetization for **3**(a) and **4**(b) at K.

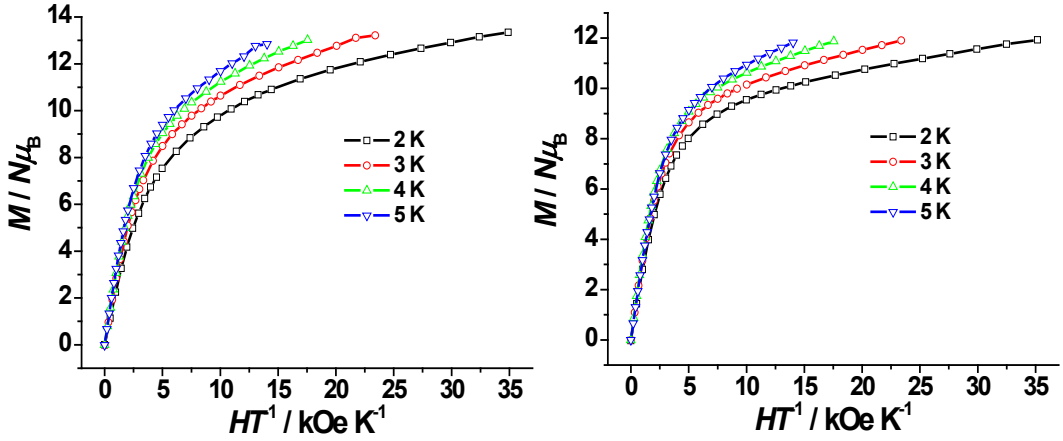

Fig. S9**.** *M* vs *H*/*T* plots at different temperatures **3**(a) and **4**(b).

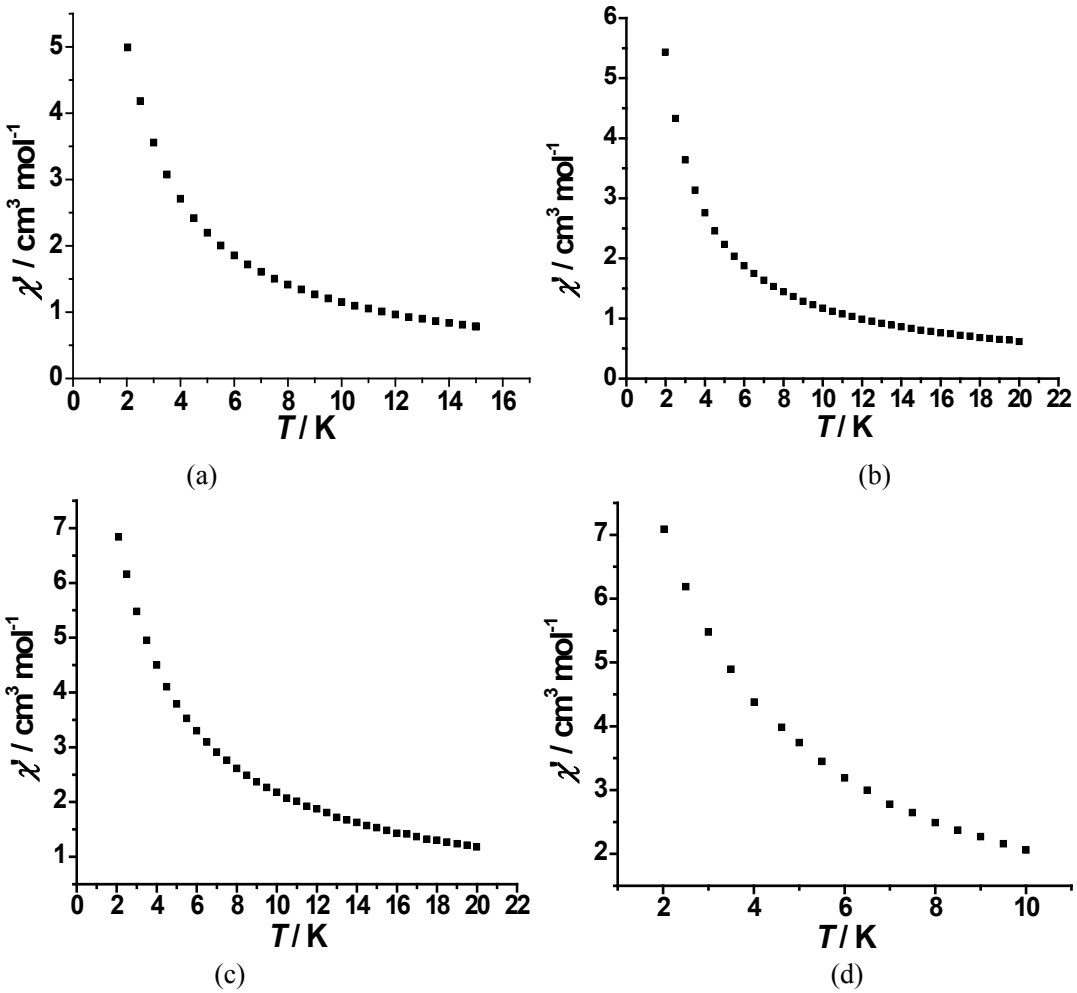

Fig. S10**.** Variable-temperature AC magnetic susceptibilities (in-phase) of complex **1**-**4** (a-d) in zero applied direct current field and an ac field of 5 Oe with a constant frequency of 997 Hz.

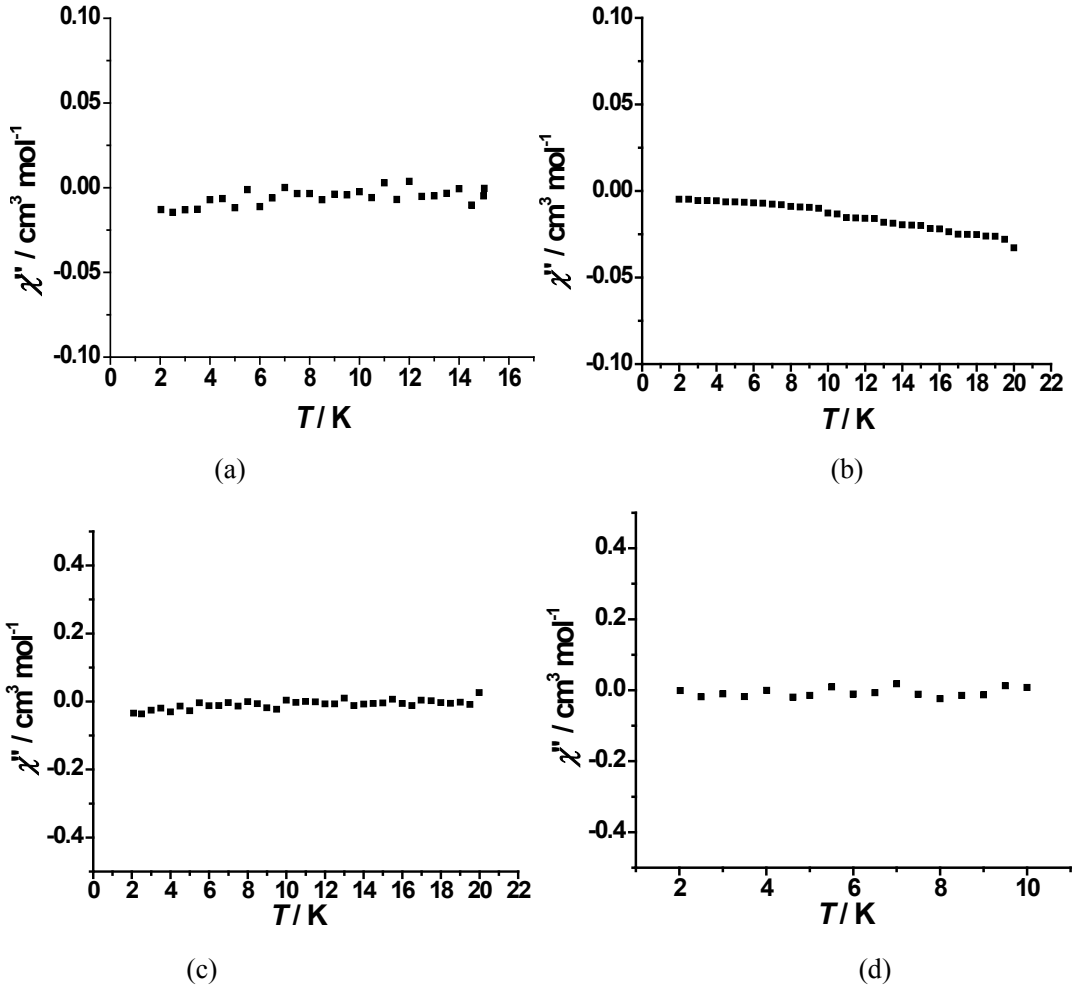

Fig. S11. Variable-temperature AC magnetic susceptibilities (out-of-phase) of complex **1**-**4** (a-d) in zero applied direct current field and an ac field of 5 Oe with a constant frequency of 997 Hz.

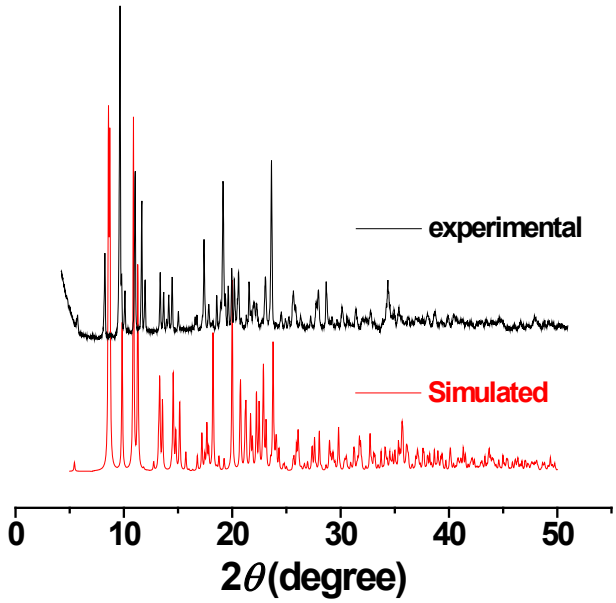

(a)

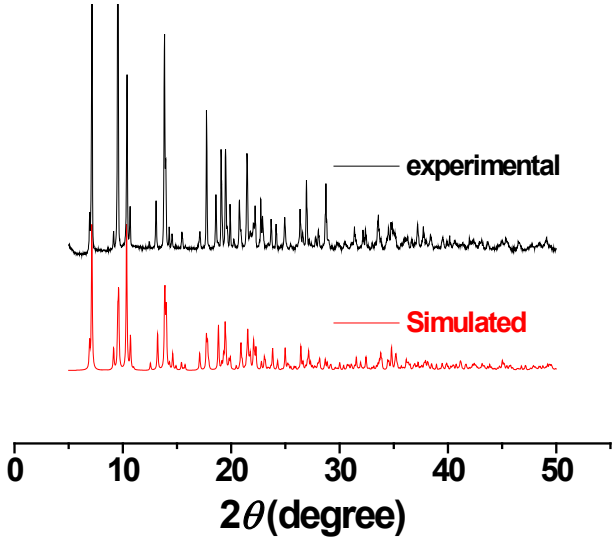

(b)

Fig. S12**.** Simulated (blue) and experimental (black) and powder XRD data for complex **1** and **3** (Because of isomorphous nature of complexes only complexes **1** and **3** were measured).